JOURNAL OF MATERIALS SCIENCE **37** (2002) 1461 – 1471

Improvement of age-hardening process of a nickel-base superalloy, IN738LC, by induction aging

S. H. RAZAVI, SH. MIRDAMADI
Department of Materials & Metallurgical Engineering, Iran University of Science & Technology (IUST), Tehran, Iran
E-mail: hrazavi@mail.iust.ac.ir

J. SZPUNAR
Department of Mining & Metallurgical Engineering, McGill University, Montreal, Qc, Canada

H. ARABI
Department of Materials & Metallurgical Engineering, Iran University of Science & Technology (IUST), Tehran, Iran

Influences of induction heating on the age-hardening process of a Nickel-base cast superalloy, IN738LC, was investigated. In this study cast specimens were undergone a solution treatment process in an argon atmosphere controlled furnace at 1125°C for 2 hours. Then, they were quenched in oil to room temperature to obtain supersaturated solid solution. These samples then subjected to two types of aging with equal heating rate, 30°C/Sec. One was induction aging and the other salt bath aging. Effects of these types of aging on the structure were analyzed and compared with normal aging having an average heating rate of 400°C/hr. The age-hardening behavior and microstructural characteristics were studied by hardness testing, scanning electron microscopy (SEM), electron image analyzing, X-ray diffractometery (XRD) and transmission electron microscopy (TEM) with replica method. According to the results obtained by these experiments, although the rate of heating of the specimens in induction and salt bath aging were equal, the diffusion-control process of nucleation and growth of γ' precipitates in induction aging were considerably accelerated. Furthermore, desirable characteristics of γ' precipitates were achieved in induction aging at lower time and temperature in comparison with times and temperatures of other types of aging. Improvement of microstructural characterization obtained in induction aging was related to the existence of an external electromagnetic force produced by induction heating. This electromagnetic force raised the effective driving force necessary for age-hardening process and intensified the nucleation and growth of γ' precipitates remarkably.

1. Introduction

Over the past decades, significant advances have been made in the development of new heat-treatment processes for superalloys to provide capability of operating at high service temperatures. In order to function satisfactorily in more severe environments, superalloys must possess properties such as outstanding high temperature strength, creep and fatigue resistance, excellent ductility, good impact resistance and adequate resistance to hot corrosion.

Cast Nickel-base superalloys are usually composed of high volume fractions of γ' phase coherently precipitated in a face-centered cubic (FCC) matrix, together with eutectic phases and one or more carbide phases. The desired properties and resistance to microstructural changes at high temperatures in these alloys are obtained by all phases with suitable structure, shape, size and distribution.

Among all the microstructural factors, the γ' precipitate morphology plays an important role in influencing the properties of Nickel-base superalloys. Actually the strength of Nickel-base superalloys is mostly related to the interactions between γ' particles and structural defects such as moving dislocations. γ' particles, Ni3(Al, Ti), have an ordered structure of Cu3Au type. Nickel atoms occupy the centers of the cube faces, with aluminum and titanium atoms at the corners of the cube. The shearing of γ' particles by a $1/2\langle 110\rangle$ matrix dislocation generates an anti-phase boundary (APB) which is removed by the passing of a second dislocation of the same burgers vector. The deformation mechanism involving the shearing of these particles is

dominant when particles are sufficiently close. Thus, the composition, size and distribution of the constituent phases particularly γ' phase control the mechanical properties of the alloys [1]. The morphology of the γ' precipitates during age-hardening treatments evolves from different mechanisms; (I) competitive growth in order to reduce the specific area of the γ–γ' interface (Ostwald ripening) and (II) shape changes in order to minimize the sum of interfacial and elastic interaction energies [2]. It has been observed that in general the precipitate growth following a $(\text{time})^{1/3}$ power law concerning diffusion controlled particle growth is in agreement with the LSW theory of Lifshitz and Slyozov [3] and Wagner [4], which was then modified by Ardell [5].

This so-called modified LSW (MLSW) theory, which was formulated for the purpose of estimating the effect of precipitate volume fraction, ϕ, on the coarsening behavior, predicts that the average particle radius, $\langle r \rangle$, should increase with time, t, according to the equation:

$$\langle r \rangle^3 - \langle r_0 \rangle^3 = Kt \tag{1}$$

where $\langle r_o \rangle$ is the average radius at the onset of coarsening and K is a volume fraction dependent rate constant given by

$$K = \frac{6\gamma D c_e \Omega^2 \langle u \rangle^3}{\nu RT} \tag{2}$$

where

$$u = r/r^* \tag{3}$$

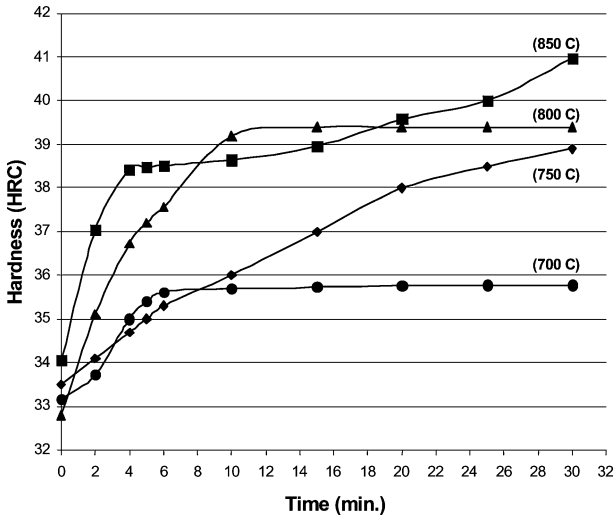

Figure 1 The hardness-time curves after salt bath aging at different temperatures.

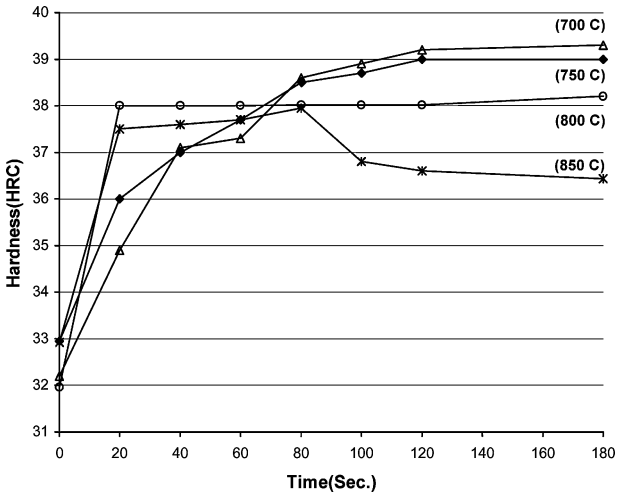

Figure 2 The hardness-time curves after induction aging at different temperatures.

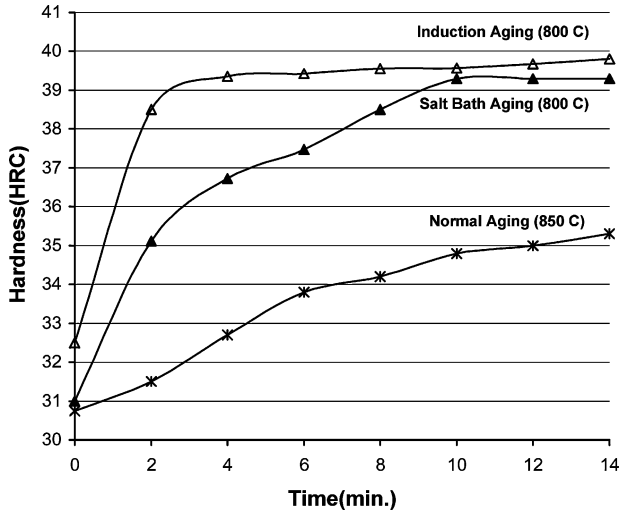

Figure 3 Comparison between the hardness-time curves of induction, salt bath and normal aging.

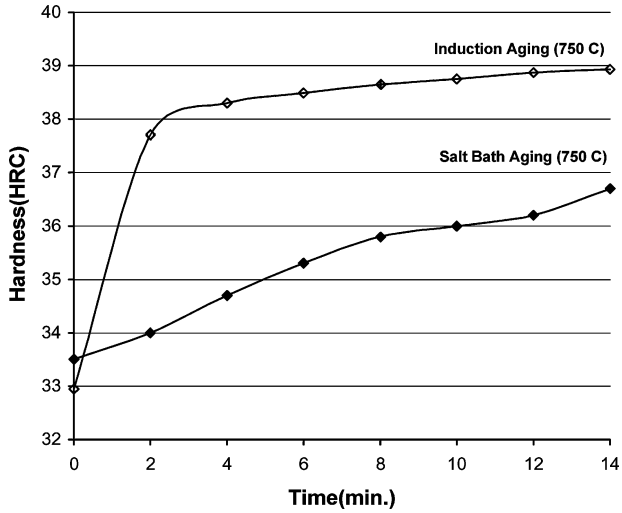

Figure 4 Comparison between the hardness-time curves of induction and salt bath aging.

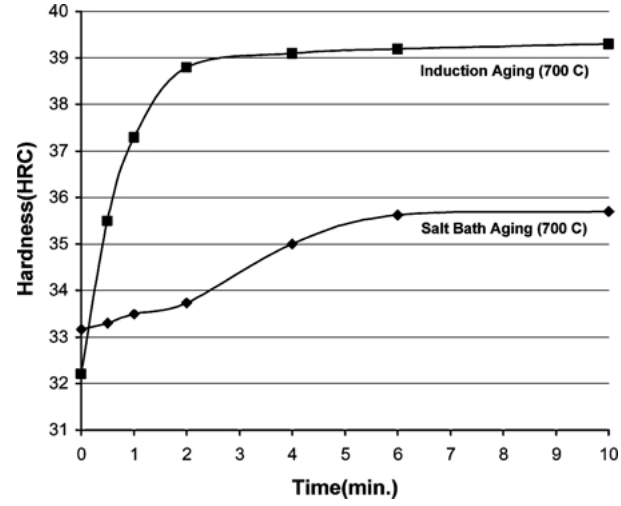

Figure 5 Comparison between the hardness-time curves of induction and salt bath aging.

$$\nu = \frac{3u_m^2}{1 + 2\beta\, u_m - \beta} \tag{4}$$

$$\beta = \frac{6\phi^{1/3}}{e^{8\phi}\Gamma(\phi)} \tag{5}$$

$$\Gamma(\phi) = \int_{8\phi}^{\infty} x^{-2/3}\, e^{-x}\, dx \tag{6}$$

The symbols in Equations 2 to 6 are defined in Table I [6].

Almost all of the studies show that the nucleation and growth of γ' precipitates in Nickel-base superalloys is diffusion controlled [7–9]. On the other hand, theoretical analysis and experimental researches show that external elastic and thermoelastic stresses affect the diffusion controlled processes [10]. According to these studies, elastic stresses affect the diffusion in ways similar to those of a pressure; the stress changes the atomic jump frequencies and biases the direction of those jumps. Stress also affects the diffusion (or chemical) potentials of the components. This implies, assuming mass flow results from a gradient in the diffusion potential, that a gradient in the stress field can induce mass flow even when the composition field is spatially uniform [10–13].

TABLE I Definitions of the symbols used in the text

γ	Interfacial free energy of the particle-matrix interface
Ω	Molar volume of the precipitate
C_e	Solubility in equilibrium with a particle of infinite size
D	Coefficient of solute diffusion in the matrix
R	Universal gas constant = 1.987 cal/mole-K
T	Absolute temperature of isothermal aging
r^*	Critical particle radius
u_m	Maximum reduced particle size of the theoretical distribution function

It has been also discovered [14] experimentally that rapid heating from room temperature to 0.8–0.9 of the melting point of alloys can enhance diffusion as well. According to these investigations, diffusion acceleration during rapid heating is explained by creating a great quantity of none-equilibrium vacancies by dislocations climbing under thermal stresses and by dense vacancy flux due to the stress gradient [14–18].

In most researches until now, resistance heating has been used for rapid heating of alloys [16, 17, 19, 20], but in this work induction heating has been chosen and the influence of electromagnetic force on age-hardening process has been investigated.

The electromagnetic field, produced by induction heating, applies an electromagnetic force on heated specimens. This force can be calculated by Maxwell's stress method [21–26]. The force adds to thermal

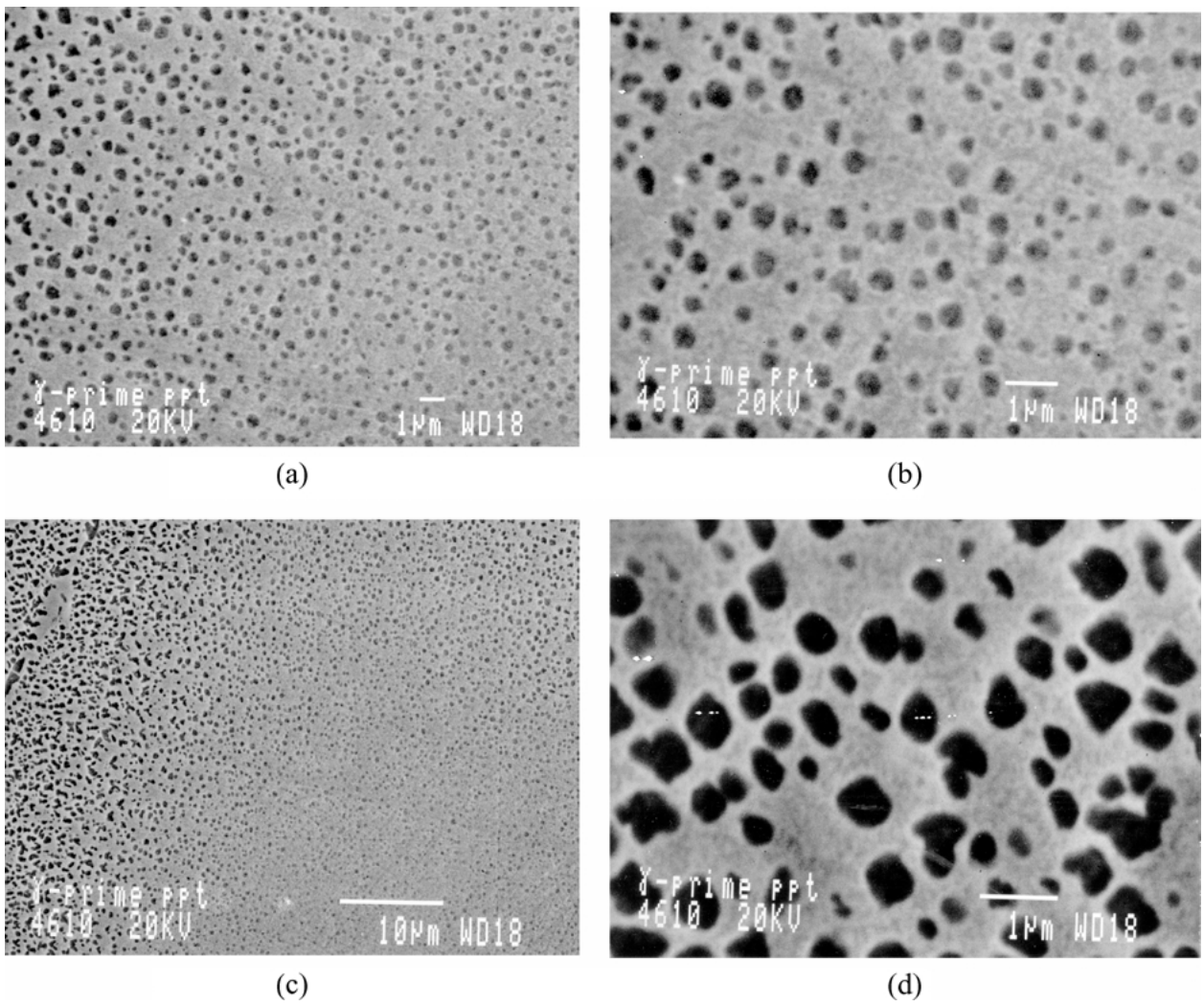

Figure 6 Microstructure of specimens obtained by SEM after induction aging at: (a) 750°C for 2 min. (b) 750°C for 15 min. (c) 800°C for 2 min. and (d) 800°C for 15 min.

stresses of rapid heating and accelerates the diffusion processes [27–28] such as nucleation and growth of secondary phases in diffusion controlled age hardening treatments.

In the present work, a Nickel-base cast superalloy was chosen and two types of rapid heating, salt bath aging and induction aging, were conducted on specimens. The results were compared with those obtained on samples that were heated gradually during the normal age-hardening process.

The age-hardening behavior and microstructural characteristics of these specimens were investigated by hardness testing, scanning electron microscopy (SEM), electron image analyzing, X-ray diffractometery (XRD) and transmission electron microscopy (TEM).

2. Experimental procedure

Several bars of IN738LC were investment casted in a vacuum furnace, then smaller specimens with dimensions of $7 * 7 * 7$ mm were cut from them. Nominal chemical composition of the investigated alloy is presented in Table II. All of the specimens were solution treated at 1125°C for 2 hours in an argon atmosphere controlled furnace and quenched in oil from 1125°C to room temperature. Subsequently, they were subjected to aging treatment by using the following three methods:

TABLE II Nominal chemical composition of used superalloy (IN738LC)

Element	Ni	Cr	Co	Mo	W	Ta	Cb	Al	Ti	C	B	Zr
Percent wt%	61.6	16.0	8.5	1.71	2.6	1.7	0.9	3.41	3.41	0.11	0.01	0.05

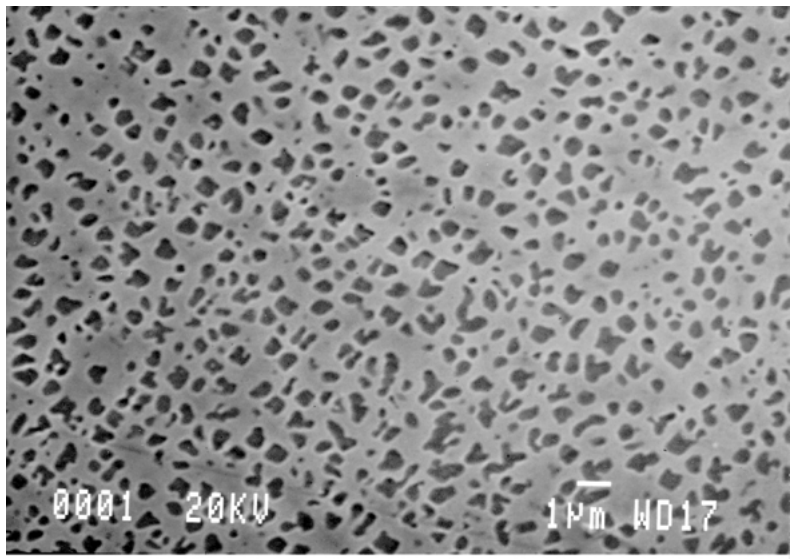

(a)

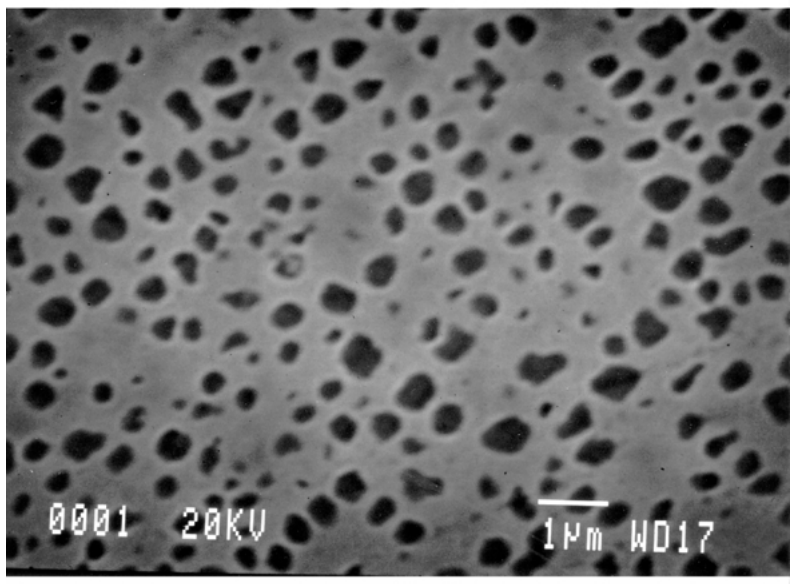

(b)

Figure 7 Microstructure of specimens obtained by SEM after salt bath aging at: (a) 800°C and (b) 850°C for 60 min.

1. Aging of specimens in high temperature salt bath at 700, 750, 800 and 850°C for 10, 20, 30 and 60 minutes. (Heating rate = 30°C/Sec.)

2. Aging of specimens with a controlled argon atmosphere medium frequency induction furnace at 700, 750, 800 and 850°C for 0.5, 1, 2 and 15 minutes. (Heating rate = 30°C/Sec.)

3. Aging of specimens in a furnace with a gradual heating rate (Normal aging with average heating rate = 400°C/hr.) and a controlled atmosphere at 850°C for 1, 2, 3 and 4 hours.

Sensitive thermocouples were spot welded to the specimens for measuring the exact temperature during aging process. The heating rate, temperature and time of aging treatment of specimens in induction furnace were programmed and controlled by an electronic programmable device, which was connected precisely to the induction furnace and thermocouples.

The hardness of samples was measured during all stages of heat treatments at room temperature by using the HRC method and the hardness curves obtained using the three methods were compared.

The specimens were then chemically etched in a solution of 2 gr. $CuCl_2$, 50 ml HCl, 25 ml HNO_3 in 200 ml H_2O for 40 seconds. Microstructure was examined by scanning electron microscope and the γ' precipitates were characterized by using electron image analyzer. In this stage, the number, area, size, aspect ratio and volume fraction of γ' precipitates were measured in all samples and the results obtained by the three methods were compared.

Transmission electron microscopy with replica method was also used for observation and analysis of very fine γ' particles, which were produced during the aging process. In addition to these tests, X-ray diffractometery was conducted on specimens after the aging processes and the diffraction patterns of samples obtained during growth of γ' precipitates were compared.

3. Results and discussion

3.1. Hardness tests

The hardness-time curves for salt bath aging (method I) and induction aging (method II) at different temperatures are shown in Figs 1 and 2, respectively. Also the comparison between the applied methods are shown in Figs 3 to 5. It can be seen that the increase of hardness in induction aging was more pronounced and faster than the two other methods specially in the first two minutes of the aging process.

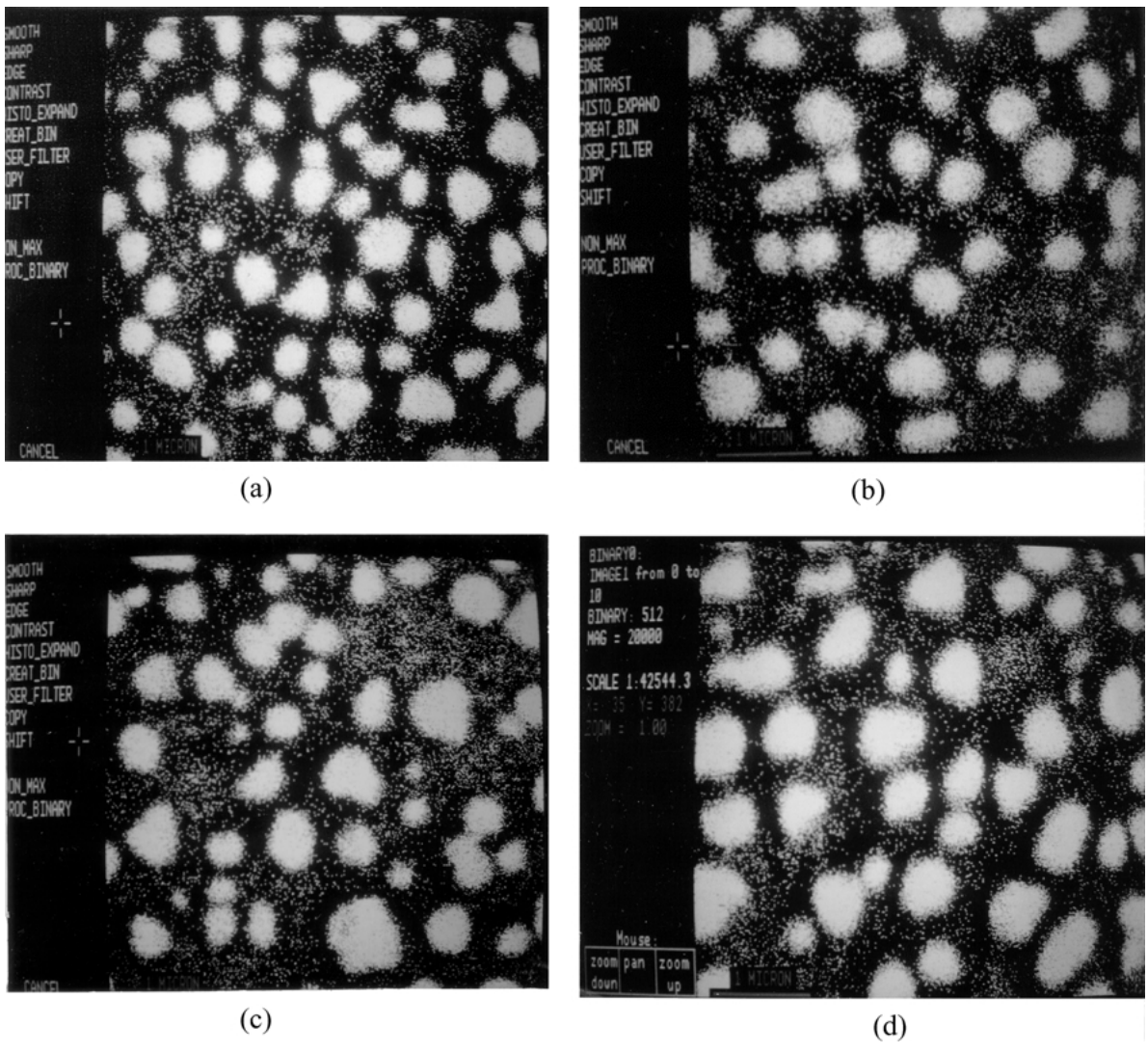

Figure 8 Microstructure images obtained by electron image analyzer after induction aging at: (a) 700°C (b) 750°C (c) 800°C and (d) 850°C for 15 min. before image filtering (×15000).

The increasing rates of hardness for salt bath aging were approximately 0.0075 HRC/Sec. For 700 and 750°C, and 0.02 HRC/Sec. for 800 and 850°C in the first minutes of aging. But these rates in induction aging were approximately, 0.12 HRC/Sec. for 700 and 750°C; 0.3 HRC/Sec. for 800°C and 0.225 HRC/Sec. for 850°C in the first 40 seconds, and after one minute, the curves obtained at lower temperatures approached upper hardness levels. The hardness of specimens at 850°C induction aging temperature began to decrease after 90 seconds of the aging process. The increasing rate of hardness was approximately 0.0086 HRC/Sec. for normal aging at 850°C in the first stages of aging (Fig. 3). Therefore, Fig. 3 shows that the increase of hardness in induction aging was higher and faster than in the two other methods even when aging is conducted at lower temperatures.

The hardness versus time curves shows that although the rate of heating of the specimens in induction and salt bath aging were the same, it seems that the nucleation and growth of precipitates in induction aging was accelerated, especially in the first minutes of aging process.

3.2. SEM and image analyzing tests

SEM photos were taken for all specimens, heat treated using the three methods listed before. A typical SEM micrograph of specimens after induction aging at 750 and 800°C for 2 and 15 minutes, and salt bath aging at 800 and 850°C for 60 minutes are shown in Figs 6 and 7, respectively.

The γ' precipitation distribution was characterized by using the electron image analyzer. The images of samples after induction aging at 700, 750, 800 and 850°C for 15 minutes before filtering are shown in Fig. 8. The images after filtering are shown in Fig. 9. Volume fractions of precipitates, number per μm^2 and mean size of γ' precipitates after induction aging at different times and temperatures are listed in Table III. Also the images of samples after salt bath aging at 700, 750, 800 and 850°C for 60 minutes and normal aging at 850°C for 240 minutes are shown in Fig. 10. Volume fractions, number per μm^2 and mean size of γ' precipitates at different times and temperatures obtained after using these two methods and filtering the image are listed in Tables IV and V, respectively.

Analysis of microstructure of the specimens after induction aging shows that γ' precipitates are fine, dispersed and almost spherical or cubic shaped and are randomly distributed in the structure of the superalloy. Two kinds of γ' can be identified in the microstructure, larger precipitates with approximately 400 ± 100 nm diameter and very fine and dispersed that have

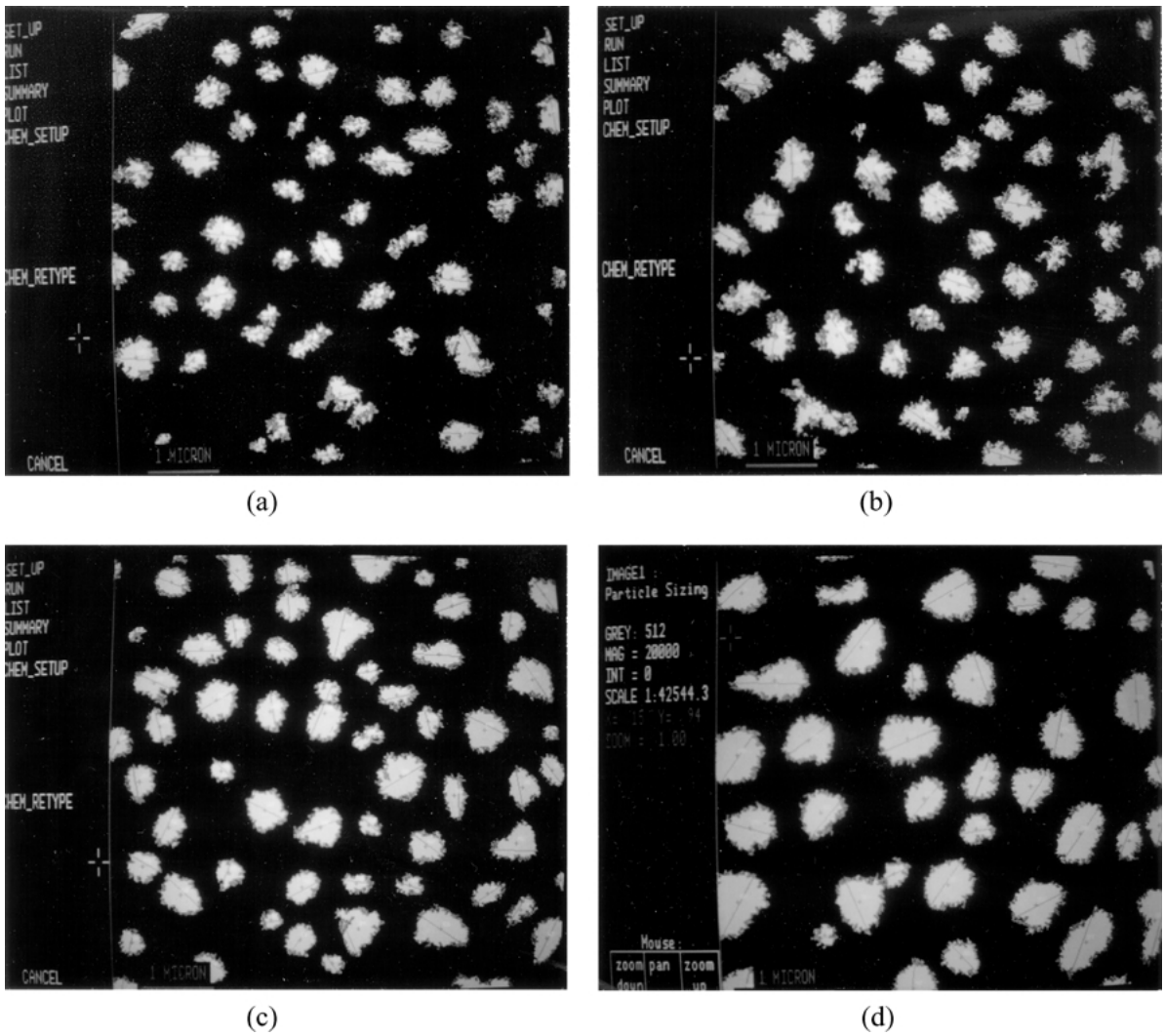

Figure 9 Microstructure images obtained by electron image analyzer after induction aging at: (a) 700°C (b) 750°C (c) 800°C and (d) 850°C for 15 min. after image filtering (×15000).

TABLE III Characteristics of primary γ' precipitates after Induction aging and filtering with electron image analyzer

Temperature of aging (°C)	Time of aging (min.)	Number of precipitates at 100 $(\mu m)^2$ field area	Mean size (diameter) (nm)	Volume fraction (%)	Aspect ratio
700	0.5	172 ± 20	297.5 ± 40	13.9	1.19
700	1	176 ± 20	357.4 ± 40	20.3	1.22
700	2	195 ± 20	396.2 ± 40	22.5	1.24
700	15	195 ± 20	449.1 ± 40	27.7	1.23
750	0.5	172 ± 20	294.5 ± 40	13.9	1.25
750	1	190 ± 20	346.7 ± 40	20.6	1.23
750	2	204 ± 20	375.4 ± 40	25.6	1.26
750	15	208 ± 20	412.7 ± 40	30.6	1.25
800	0.5	176 ± 20	300.5 ± 40	14.3	1.27
800	1	195 ± 20	345.1 ± 40	23.9	1.25
800	2	213 ± 20	380.9 ± 40	26.2	1.28
800	15	222 ± 20	428.8 ± 40	32.5	1.27
850	0.5	172 ± 20	339.9 ± 40	15.8	1.26
850	1	176 ± 20	398.1 ± 40	20.8	1.29
850	2	181 ± 20	462.8 ± 40	24.4	1.27
850	15	181 ± 20	483.9 ± 40	24.9	1.29

TABLE IV Characteristics of primary γ' precipitates after salt bath aging and filtering with electron image analyzer

Temperature of aging (°C)	Time of aging (min.)	Number of precipitates at 100 $(\mu m)^2$ field area	Mean size (diameter) (nm)	Volume fraction (%)	Aspect ratio
750	10	127 ± 20	336.8 ± 40	12.4	1.23
750	20	145 ± 20	346.2 ± 40	14.4	1.27
750	30	163 ± 20	376.8 ± 40	18.1	1.31
750	60	167 ± 20	429.9 ± 40	25.7	1.29
800	10	145 ± 20	340.5 ± 40	12.8	1.33
800	20	167 ± 20	351.2 ± 40	15.3	1.30
800	30	190 ± 20	385.3 ± 40	22.1	1.35
800	60	195 ± 20	424.1 ± 40	25.3	1.38
850	10	167 ± 20	334.6 ± 40	13.0	1.36
850	20	176 ± 20	359.3 ± 40	18.4	1.38
850	30	190 ± 20	389.3 ± 40	23.0	1.40
850	60	199 ± 20	437.3 ± 40	27.4	1.42

TABLE V Characteristics of primary γ' precipitates after normal aging and filtering with electron image analyzer

Temperature of aging (°C)	Time of aging (min.)	Number of precipitates at 100 $(\mu m)^2$ field area	Mean size (diameter) (nm)	Volume fraction (%)	Aspect ratio
850	60	186 ± 20	363.9 ± 40	20.1	1.45
850	120	195 ± 20	410.9 ± 40	26.1	1.47
850	180	195 ± 20	448.7 ± 40	33.0	1.42
850	240	176 ± 20	508.1 ± 40	34.9	1.44

TABLE VI Characteristics of ultrafine secondary γ' precipitates after induction aging before filtering with electron image analyzer

Temperature of aging (°C)	Time of aging (min.)	Number of precipitates at 1 $(\mu m)^2$ field area	Mean size (diameter) (nm)	Volume fraction (%)	Aspect ratio
750	2	1600 ± 100	20 ± 10	28.8	1.21

approximately 20 ± 10 nm diameter. The number of very fine and dispersed γ' phase precipitates were around 1600 ± 100 per $(\mu m)^2$. A summery of characterization of precipitates for a randomly selected area of a sample undergone 750°C induction aging for 2 minutes is presented in Table VI. One should emphasize that during the standard age-hardening process of IN738LC (850°C for 24 hr.) these characteristics are obtained after 24 hours, achieving better characterizations of γ' phase by induction aging at 700 to 800°C for under 15 minutes is a very impressive result.

Study of the results of electron image analysis indicates that in the induction aging process, the increase of time in a certain temperature results in:

- The increase of the size of precipitates
- The increase in the volume fraction of precipitates in the first stages of the aging process and tending

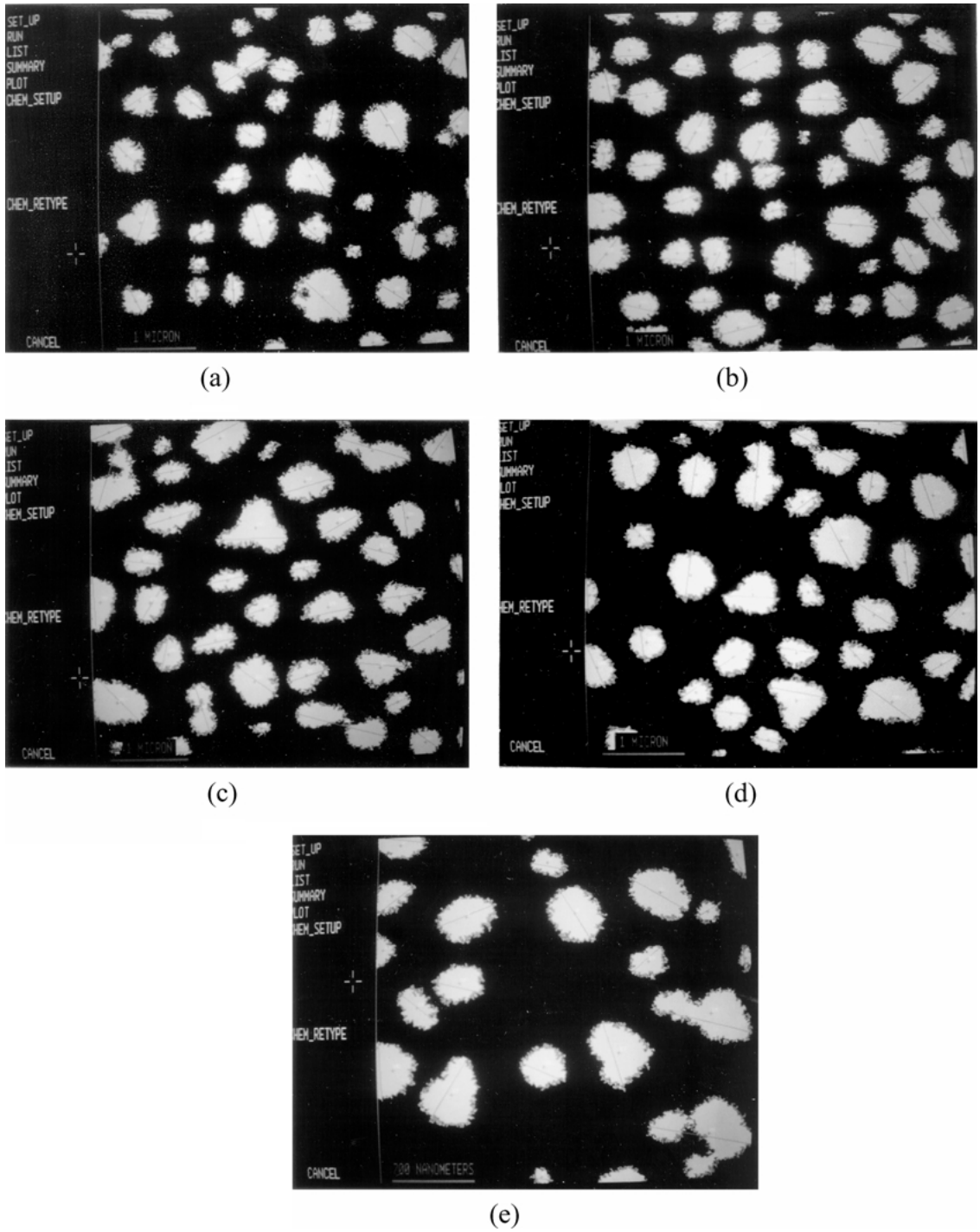

Figure 10 Microstructure images obtained by electron image analyzer after salt bath aging at: (a) 700°C (b) 750°C (c) 800°C and (d) 850°C for 60 min., and normal aging at: (e) 850°C for 240 min.(×15000).

to a constant value over the course of time at higher temperatures
- The slight increase in the number of precipitates per unit volume of specimens, in the first stages of the aging process and tending to a constant value over the course of time.

According to these induction-aging tests, the increase of temperature in a certain time results in:

- The approximate constancy of the size of precipitates, considering standard deviation, below the critical temperature and their coarsening above it.
- The increase of the volume fraction of precipitates below critical temperature and the decrease of the volume fraction above it; for example, at 850°C the induction aging process after 2 minutes, although precipitates were larger in comparison with lower temperatures, the volume fraction and hardness of precipitates were lower. It shows that the critical temperature of aging in the induction method is around 850°C.
- The slight increase in the number of precipitates, considering standard deviation, below critical temperature and the decrease in numbers above it.

It is known that in all of the age-hardening processes there is a critical temperature and time to which the further increase of them causes the decrease of the mechanical properties of alloys due to unwanted

changes in volume fraction, size, number, shape, distribution and other characteristics of secondary phases. The amount of these critical parameters depends on the total energies or forces applied to specimens during the aging process. In induction aging, due to presence of an extra electromagnetic force, these critical parameters move to lower amounts in comparison with salt bath and normal aging. The results of SEM and image analysis obtained from 700 to 800°C induction aging were better than upper temperatures. The characteristics of precipitates tended to undesirable values with the further increase of the aging temperature to 850°C.

In salt bath aging due to the absence of electromagnetic force, the critical time and temperature move to upper levels. The results obtained indicate that the size, number and other characteristics of precipitates tended to be better and have more desirable values with the increase of the aging temperature from 700 to 850°C. It worth mentioning that at higher temperatures the morphology of precipitates starts to change gradually from spherical and cubic toward incoherent morphologies.

Of course the rules mentioned before about the changing of the volume fraction, size and number of precipitates with the increase of temperature in constant time and inverse, are also valid for salt bath and normal aging. But, in general, in induction aging the desirable characteristics of γ' precipitates were achieved in lower temperatures and times than the other two methods. For example, the results of 700 to 800°C induction aging for 15 minutes were so much better than the results of 850°C salt bath and normal aging for 60 and 240 minutes respectively.

3.3. TEM tests

Transmission Electron Microscopy tests by replica method were done on specimens after induction aging. TEM micrographs of samples after 700°C induction aging for 15 minutes and 750°C for 2 and 15 minutes are shown in Fig. 11. Also X-ray analysis of very fine γ' precipitates which were done along with TEM tests is presented in Fig. 12.

It can be seen that after only two minutes aging at 750°C with induction heating, so many fine and dispersed γ' precipitates with 20 ± 10 nm diameter were produced (Re. Table VI) and nucleation was remarkable all over the sample especially around larger γ' phases due to their surface energy. According to the TEM micrograph of specimens after 15 minutes aging at 750°C, the very fast growth of these ultrafine γ' precipitates is also evident. Even at 700°C induction aging (150°C less than the normal aging temperature) the speed of nucleation and growth of γ' precipitates was considerable.

The X-ray analysis during TEM tests confirmed that these fine and dispersed precipitates were γ' (Ni3(Al,Ti)) phase.

3.4. XRD tests

A typical X-Ray Diffractometery graph of a specimen after 750°C induction aging for 15 minutes is shown in Fig. 13. The intensity of Ni3(Al,Ti) phase picks

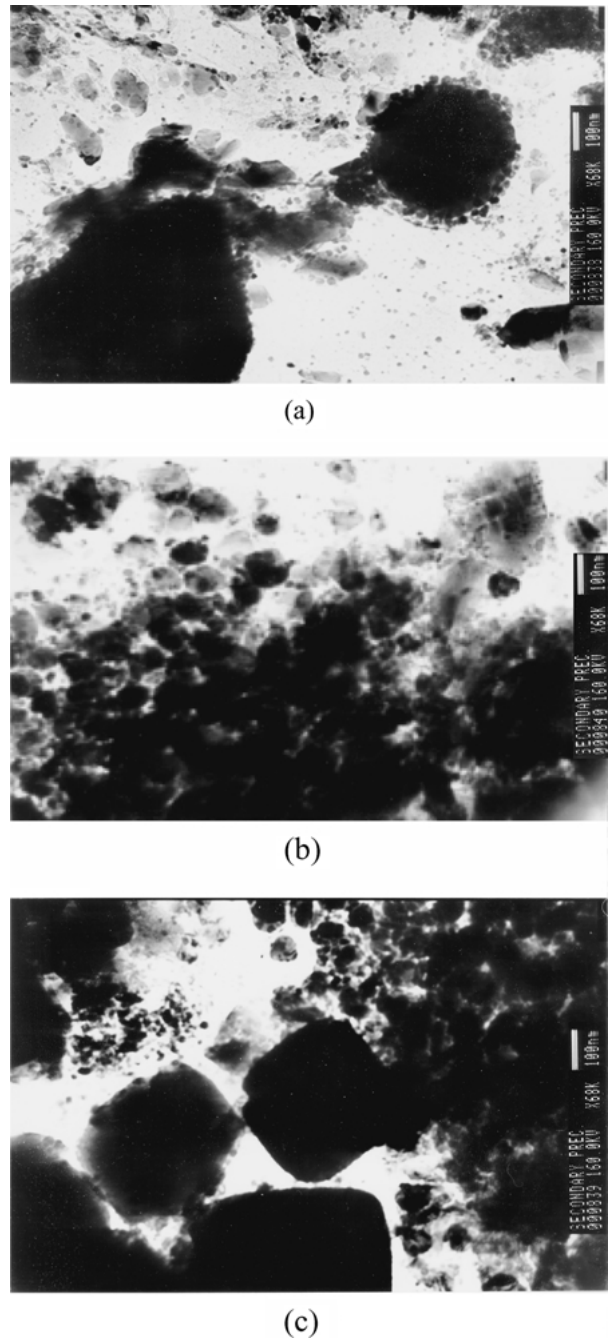

Figure 11 Microstructure of specimens obtained by TEM after induction aging at: (a) 750°C for 2 min. (b) 750°C for 15 min. and (c) 700°C for 15 min.

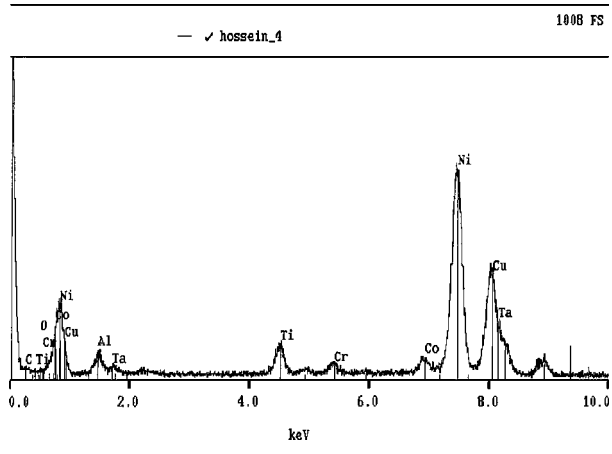

Figure 12 X-ray analysis of ultrafine γ' precipitates, which obtained during TEM tests.

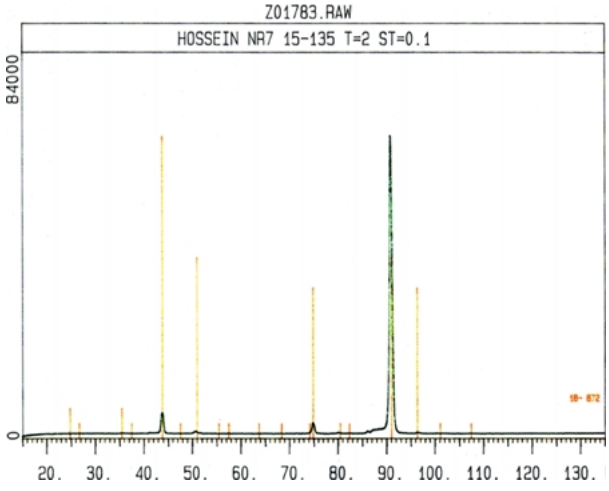

Figure 13 X-ray diffractometery (XRD) of a specimen after induction aging at 750°C for 15 min.

(18-872 card no.) was very considerable which surpassed the picks of other phases.

4. Conclusion

In the present study two types of rapid heating, induction aging and salt bath aging, were conducted on a chosen Nickel-base cast superalloy and the results were analyzed and compared with gradual heating of this superalloy during the normal age-hardening process. The age-hardening behavior and microstructure characteristics were studied by hardness testing, scanning electron microscopy (SEM), electron image analyzing, X-ray diffractometery (XRD) and transmission electron microscopy (TEM) with replica method.

The results are summarized as follows:

1. The increasing rate of hardness in induction aging was more pronounced and faster than the two other methods especially in the first two minutes of aging process.

2. The hardness-time curves of salt bath aging went to upper levels with the increase of temperature.

3. In the hardness-time curves of induction aging, the curves of lower temperatures (700 and 750°C) went to upper levels after one minute of the aging process in comparison with higher temperatures (800 and 850°C). Even the hardness of specimens at 850°C induction aging began to decrease after 90 seconds of aging process.

4. The results of SEM and electron image analyzing obtained from 700 to 800°C induction aging were better than 850°C. But in salt bath aging, the characteristics of precipitates tended to better and more desirable values with the increase of the aging temperature from 700 to 850°C. It shows that the induction aging, due to presence of an extra electromagnetic force, the critical temperature and time for changing characteristics of γ' phase toward undesirable values moved to lower amounts in comparison with salt- bath and normal aging.

5. Microstructure study of samples with SEM and TEM tests after induction aging shows that the rate of nucleation and growth of γ' precipitates in the first minutes of aging process were extraordinarily high and remarkable in comparison with the two other methods.

6. Microstructure of the superalloy samples after induction aging at 750°C for 2 minutes contained very fine secondary γ' with: average diameter of 20 ± 10 nm, approximately 1600 ± 100 particles per $(\mu m)^2$ area, aspect ratio around one (spherical shape), high volume fraction (28.8%) and random distribution in microstructure.

7. The X-ray analysis during TEM tests confirmed that the fine and dispersed secondary phase in microstructure of experimented specimens was γ' (Ni3(Al, Ti)) phase.

8. Although the rate of heating of the specimens in induction and salt bath aging were equal, the diffusional process of nucleation and growth of γ' precipitates in induction aging were accelerated so much especially in the first minutes of aging process. In general, in induction aging the desirable characteristics of γ' precipitates are achieved in lower temperatures and times than salt bath and normal aging.

9. The electromagnetic field, produced by induction heating, applied an electromagnetic force on heated superalloy specimens, and this force added to the thermal stresses of rapid heating and remarkably accelerated the diffusional process of nucleation and growth of γ' precipitates.

Acknowledgment

The assistance of the following people in various aspects of the experimental work is greatly appreciated: Dr. Valli for TEM tests, M. Sc. H. Campbel for SEM tests, Mr S. Poplawsky for technical assistance, members of the Texture Lab and the Hot Deformation Lab in the Mining & Metallurgical Engineering Department of McGill University and the materials and metallurgical school of Iran University of Science & Technology.

References

1. N. NJAH and O. DIMITROV, *Acta Metall.* **37**(9) (1989) 2559.
2. H. T. KIM, S. S. CHUN, X. X. YAO, Y. FANG and J. CHOI, *J. Mater. Sci.* **32** (1997) 4917.
3. I. M. LIFSHITZ and V. V. SLYOZOV, *J. Phys. Chem. Solids* **19** (1961) 35.
4. C. WAGNER, *Z. Elektrochem.* **65** (1961) 581.
5. A. J. ARDELL, *Acta Met.* **20** (1971) 61.
6. D. J. CHELLMAN and A. J. ARDELL, *Acta Metall.* **22** (1974) 577.
7. A. GES, H. PALACIO and R. VERSACI, *J. Mater. Sci.* **29** (1994) 3572.
8. T. GROSDIDIER, A. HAZOTTE and A. SIMON, *Materials Science and Engineering* A **256** (1998) 183.
9. M. F. HENRY, Y. S. YOO, D. Y. YOON and J. CHOI, *Metallurgical Transactions* A **24A** (1993) 1733.
10. W. C. JOHNSON, *Metallurgical and Materials Transactions* A **28A** (1997) 27.
11. W. HORT and W. C. JOHNSON, *ibid.* **27A** (1996) 1461.
12. W. C. JOHNSON, *Zeitschrift fur Physikalische Chemie* **Bd. 206** (1998) 165.
13. W. HORT and W. C. JOHNSON, *Scripta Materialia* **34**(7) (1996) 1015.
14. M. V. YARMOLENKO, Defect and Diffusion Forum **143–147** (1997) 1613.
15. *Idem.*, *ibid.* **129–130** (1996) 321.

16. H. MATZNER and M. H. BRAUNAU, *Aluminium* **73** (1997) 214.
17. V. V. MEDVEDEV, YU. B. SAZONOV and S. A. KONSTANTINOVA, *Steel in the USSR* **15** (1985) 442.
18. A. G. RAKHSHTADT, O. M. ZHIGALINA, O. M. KHOVOVA and G. M. KLYKOV, *The Physics of Metals and Metallography* **81**(5) (1996) 557.
19. F. S. EPSTEIN and G. L. WHITE, *Chemical Engineering* (5) (1996) 112.
20. A. BARLETTA and E. ZANCHINI, *Int. J. Heat Mass Transfer* **39**(6) (1996) 1307.
21. M. ENOKIZONO, T. TODAKA, K. YOKOJI, I. MATSUMOTO, K. KUBO and Y. WADA, *IEEE Transactions on Magnetics* **31**(6) (1995) 4205.
22. M. ENOKIZONO, T. TODAKA, K. YOKOJI, Y. WADA and I. MATSUMOTO, *ibid.* **31**(3) (1995) 1869.
23. Y. KAWASE, T. YAMAGUCHI and N. HAYASHI, "Nonlinear Phenomena in Electromagnetic Fields" (Elsevier Science, Amesterdam, 1992) p. 233.
24. X. WANG, X. B. WANG and P. R. C. GASCOYNE, *Journal of Electrostatics* **39** (1997) 277.
25. V. A. SARANIN, *Technical Physics* **43**(2) (1998) 145.
26. Z. W. SHI and C. B. RAJANATHAN, *Computation in Electromagnetics* **10–12**(4) (1996) 241.
27. E. E. GLICKMAN, *Defects and Diffusion Forum* **129/130** (1996) 225.
28. I. D. KAGANOVICH, *Tech. Phys. Lett.* **19**(5) (1993) 276.

Received 17 January 2000
and accepted 17 April 2001